

Application of Taguchi Method for Characterization of IrO₂-RuO₂ Film

Kyung-Sun Chae, Hyeong-Ki Choi, Joon-Hong Ahn*,
Yo-Seung Song*, and Deuk Yong Lee**

*Biotechnology and Environmental Engineering Division, Agency for Technology
and Standards, Kwacheon 427-010, Korea*

**Department of Materials Engineering, Hankuk Aviation University
Koyang 412-791, Korea*

***Department of Materials Engineering, Daelim College of Technology
Anyang 431-715, Korea*

Ti/TiO₂/IrO₂-RuO₂ electrodes were evaluated to conduct the optimum manufacturing conditions of IrO₂-RuO₂ film with an aid of Taguchi method. The heat treatment temperature and heat treatment time with the flow rate change of air and the corrosion resistance of the electrodes were evaluated. The presence and the type of the TiO₂ intermediate layer was a critical factor to the anticorrosion properties of the Ti/TiO₂/IrO₂-RuO₂ electrodes among four different experimental parameters to be investigated. The optimal condition of the dip-coated IrO₂-RuO₂ film was the TiO₂ intermediate layer to be prepared by plasma spray and subsequently treated for 120 min at 450°C with air flow rate of 3 sccm.

Keywords : corrosion, Ti/TiO₂/IrO₂-RuO₂ electrode, Taguchi method, orthogonal array, plasma spray, dip coating

1. Introduction

It is well-known that lead zirconate titanate (PZT) ferroelectric thin films have been considered as the material of choice for microelectronic device applications such as high density dynamic random-access memory capacitors and nonvolatile memories.^{1,3-4)} Recently, the transition metal oxides having the tetragonal rutile crystal structure has been proposed as the buffer layer to avoid the interface-related fatigue degradation between PZT thin film and the metal electrode.^{1,3-4)} These transition metal oxides such as IrO₂ and RuO₂ possess versatile merit such as low bulk resistivity (30~100 μΩ-cm), excellent thermal stability, and diffusion barrier properties, which are prerequisite for the conducting materials.^{1,4)}

The effectiveness of the transition metal oxides can be extended to the electrode coating film for anticorrosion applications such as cathodic protection and to the oxygen evolving electrodes for electroflotation.⁷⁻⁸⁾ Typical example in the corrosion industry is the IrO₂-RuO₂ film on Ti electrodes used for underground pipelines and cables, gas tanks, structural fixtures, and ships, which are exposed to the severely corrosive environments.⁷⁾ For the anticorrosion efficiency of the IrO₂-RuO₂ film on Ti electrodes,

TiO₂ intermediate layer was employed by either sputtering or plasma spray to suppress the discontinuous formation of electrically insulating oxide (TiO₂) on the Ti electrode surface. The IrO₂-RuO₂ film was dip-coated and then dried for 10 min at 130°C and then annealed for 10 min at temperatures from 400 to 500°C in air.

It has been noted that Taguchi method is a powerful tool to determine the optimal condition of experimental parameters so that the performance characteristic is robust against noise factors P.⁹⁾ In addition, its efficiency in experimentation offers various advantages over the existing approaches. In the present study, electrical properties of IrO₂-RuO₂ film prepared by a dip-coating process were investigated via Taguchi method and orthogonal arrays to determine the optimal setting and the relationship of experimental variables. Experimentally, four parameters were considered as follows: (1) preparation method of intermediate layer between Ti substrate and IrO₂-RuO₂ film; (2) heat treatment temperature; (3) heat treatment time; and (4) flow rate of air. Each parameter was further subdivided into 3 levels. Then, L₉ (3⁴) orthogonal arrays were evaluated to optimize the performance characteristics of the dip-coated IrO₂-RuO₂ film.

2. Experimental procedure

The titanium substrate having a dimension of 50 × 50 × 3 mm was polished using a SiC grit of 220 and then surface treated in 6N HCl for 1 h at 90°C and distilled water. The film precursor solution was prepared by dissolution of 10mol% IrCl₃ · 3H₂O:90mol% RuCl₃ · xH₂O in isopropanol. After dip-coating, the specimen was firstly dried for 10 min at 130°C and then annealed for 10 min at temperatures from 400 to 500°C under air atmosphere (less than 1% hydrocarbon). The flow rate of air was varied from 3 to 7 standard cubic centimeter per minute (sccm). This drying process was repeated successively up to five times. Finally, dip-coated IrO₂-RuO₂ film was obtained by heat treatment for 60 to 120 min at temperatures from 400 to 500°C with 3 to 7 sccm air flow rate. TiO₂ oxide was chosen as the intermediate layer between the IrO₂-RuO₂ top-coat and the Ti substrate to improve the conduction. The intermediate layer of 3 (m and 15 (m in thickness was prepared by sputtering and plasma spray, respectively, and the experimental parameters were summarized in Table I.

Four experimental parameters are chosen and L₉(3⁴) orthogonal arrays are constructed as listed in Table II.⁹⁾ In Table II, A, B, C, and D indicate type of intermediate layer, heat treatment temperature, flow rate of air, and heat

Table 1. Experimental conditions of L₉(3⁴) orthogonal arrays

No.	A	B	C	D
1	A1	B1	C1	D1
2	A1	B2	C2	D2
3	A1	B3	C3	D3
4	A2	B1	C2	D3
5	A2	B2	C3	D1
6	A2	B3	C1	D2
7	A3	B1	C3	D2
8	A3	B2	C1	D3
9	A3	B3	C2	D1

Table 2. Plasma spray and sputtering experimental conditions

Process variable	Plasma spray	Sputtering
Primary argon gas flow rate	80 sccm	500 sccm
Secondary hydrogen gas flow rate	15 sccm	
Vacuum level		8 × 10 ⁻³ torr
Power supply level	70 A, 500 V	3 kW
Rotating speed of substrate		10 rpm
Gun-substrate spray distance	85 mm	
Powder feed rate	3 kg/h	
Gun nozzle diameter	5 mm	

treatment time, respectively. Each variable is further subdivided into 3 levels. A₁, A₂, and A₃ represent non-bonding layer, intermediate TiO₂ layer prepared by sputtering, and by plasma spray, respectively. B₁, B₂, and B₃ imply 400, 450, and 500°C. C₁, C₂, and C₃ denote 3, 5, and 7 sccm, respectively. Lastly, D₁, D₂, and D₃ express 60, 90, and 120 min, respectively. Current density of the IrO₂-RuO₂ films in Table I was related to signal to noise (S/N) ratio to determine the optimized experimental condition and to reveal the influence of adjustment parameters on corrosion resistance of the IrO₂-RuO₂ film.

Polarization cell is composed of one working electrode (insoluble anode) and two counter graphite electrodes located inside the cell.⁸⁾ One reference electrode (saturated calomel electrode, SCE) was positioned as close as possible to the working electrode. The electrochemical measurements were conducted in 3.5 wt% NaCl at 25°C and 1500 mV (SCE) with a sweep rate of 600 mV/sec according to ASTM G5-94. The potential was measured by a potentiostat in the range of the open-circuit potential to 1800 mV. The details of the potentiodynamic polarization experiment were described elsewhere.⁸⁾

X-ray diffraction (XRD, XRD-3000, Rich Seifert Co., Germany) was performed to identify the composition of the IrO₂-RuO₂ films. A scan speed of 0.05° 2θ/sec was used in the 2θ range of 20° to 80°. Microstructure of the IrO₂-RuO₂ film and the TiO₂ intermediate layer was investigated with transmission electron microscopy (TEM, FEM-2000FX II, Jeol, Japan). Also, the coatings were quantitatively characterized by scanning electron microscopy (SEM) and energy-dispersive X-ray spectroscopy (EDX).

3. Results and discussion

Experimental anticorrosion current density (j) having the properties of larger better was converted to S/N ratio according to the equation of $S/N = -10 \times \log[1/n \sum ((1/j)^2)]$, where n and j are the degree of freedom and the current density, respectively. The S/N ratio is listed in Table III. The optimal experimental condition can be achieved when the S/N ratio becomes the largest among the experiments investigated, because it is known that Taguchi analysis may give better reliability and predict the optimal processing setting under various adjustment parameter conditions.⁹⁾ The average and the contribution rate (ratio) of individual levels were calculated based on the S/N ratio and shown in Table IV. The variation of the average values of levels increased as the experimental parameters went from DRBRCRA, indicating that the influence of experimental parameters on the corrosion resistance became pro-

Table 3. S/N ratios determined by Taguchi analysis

No.	A	B	C	D	S/N ratio
1	A1	B1	C1	D1	0.0478
2	A1	B2	C2	D2	0.0444
3	A1	B3	C3	D3	0.0497
4	A2	B1	C2	D3	0.0405
5	A2	B2	C3	D1	0.0604
6	A2	B3	C1	D2	0.0571
7	A3	B1	C3	D2	0.0630
8	A3	B2	C1	D3	0.0761
9	A3	B3	C2	D1	0.0509

nounced in the order of D (0.0024) < B (0.0099) < C(0.015) < A(0.016). It suggested that the subdivided levels were directly related to the anticorrosion current density of the IrO₂-RuO₂ film, therefore, small deviation of the contribution rate having a higher value in Table IV was more susceptible to the large divergence of the current density. In the present study, the optimal test

condition having the highest contribution rate of the levels (anticorrosion current density) was A₃B₂C₁D₃ as listed in Table III. Thus, the dip-coated IrO₂-RuO₂ film having the TiO₂ intermediate layer prepared by plasma spray (A₃) and subsequently heat treated for 120 min (D₃) at 450°C (B₂) with 3 sccm air flow rate (C₁) was likely to be the optimal experimental condition (A₃B₂C₁D₃).

For the comparison between the extremes in the present study, experimental current density of the sample no. 4 (A₂B₁C₂D₃) and no. 8 (A₃B₂C₁D₃) in Table I was examined by the potentiodynamic polarization test and is depicted in Figure 1 Current density of A₂B₁C₂D₃ and A₃B₂C₁D₃ at 1500 mV (SCE) is 0.040 A/cm² and 0.076 A/cm², respectively, showing that the current density of no. 8 (> 0.05 A/cm²) is effective to the corrosion resistance.⁸⁾ Figure 2 is a TEM image of the TiO₂ intermediate layer, which demonstrates that the TiO₂ is composed of small grains. The shape and size of the TiO₂ grains ranged broadly from distorted spheres with diameters of 10(50 nm (sput

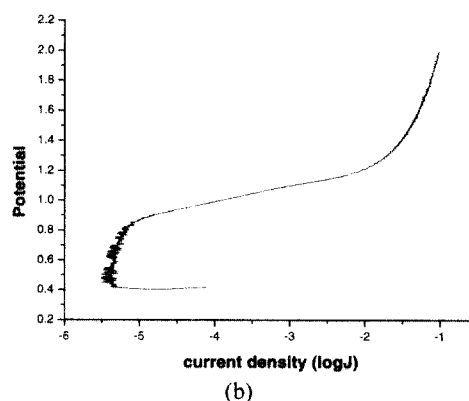
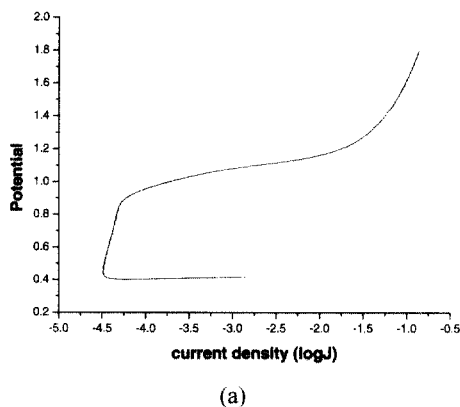
**Fig. 1.** Polarization diagram of (a) specimen no. 4 and (b) no. 8**Fig. 2.** TEM image of TiO₂ layer prepared by (a) sputtering and (b) plasma spray.

Fig. 3. TEM image of IrO₂-RuO₂ film with various air flow rate of (a) 3 sccm, (b) 5 sccm, and (c) 7 sccm.

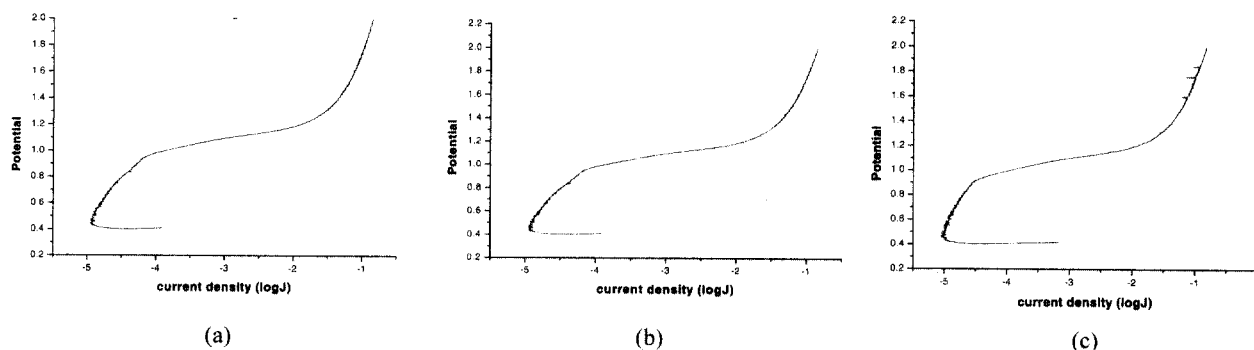


Fig. 4. Current density of IrO₂-RuO₂ electrodes as a function of potential by varying air flow rate of (a) 3 sccm, (b) 5 sccm, and (c) 7 sccm.

tering, A₂B₁C₂D₃) and platelets with diameters of 180 (240 nm (plasma spray, A₃B₂C₁D₃), respectively. Smaller grain size led to larger grain boundaries, which may act as a barrier to the current flow.⁷⁾ The conduction electrons are likely to be scattered by grain boundaries, resulting in the loss of current density. Larger grains (A₃B₂C₁D₃) of the as-plasma sprayed TiO₂ layer was obtained because plasma spraying employed a gun that simultaneously melts and propels small droplets of ceramic oxides onto the surface to be coated. Twinning was observed for the TiO₂ layer prepared by the plasma spray. It may be due to the plasma stream temperature that melts did not have enough mobility to relieve the stress generated by spray damage, resulting in deformation by twinning. Therefore, the difference in current density may be attributed to the disparity of microstructure caused by the different preparation method of the intermediate layer.

The effect of grain size on current density of the Ti/IrO₂-RuO₂ electrodes was further investigated by changing the air flow rate (C) from 3 to 7 sccm. Grain size less than

Table 4. Average and contribution rate of individual levels

Individual level	Average	Contribution rate
A1	0.0473	-7.1 × 10 ⁻⁵
A2	0.0537	-0.7 × 10 ⁻⁵
A3	0.0633	8.9 × 10 ⁻⁵
B1	0.0504	-4.0 × 10 ⁻⁵
B2	0.0603	5.9 × 10 ⁻⁵
B3	0.0525	-1.9 × 10 ⁻⁵
C1	0.0603	5.9 × 10 ⁻⁵
C2	0.0453	-9.1 × 10 ⁻⁵
C3	0.0576	3.3 × 10 ⁻⁵
D1	0.0530	-1.4 × 10 ⁻⁵
D2	0.0554	1.0 × 10 ⁻⁵
D3	0.0548	0.4 × 10 ⁻⁵

10 nm was observed for the film prepared at the air flow rate of 3 sccm as shown in Figure 3 Grain size increased from 20~40 nm to 15~80 nm and morphologies was

changed from distorted spherical grain to elongated grain as the air flow rate rose from 5 to 7 sccm. Experimental current density as a function of the flow rate of air is displayed in Figure 4. As the grain size increased, the current density started to rise and then decreased as shown in Figure 4 and Table IV. The result is in conflict with the above result, therefore, it is believed that the shape of the grains is more important than the grain size because the perimeter to diameter ratio increases and then electron mean free path increases with fewer grain boundaries as a result of the grain morphology.⁵⁾ Therefore, it is noted that the contribution of A parameter to the anticorrosion behavior is more pronounced as compared to that of C parameter.

The composition of the IrO₂-RuO₂ top-coat film was examined quantitatively using SEM/EDX as shown in Figure 5. Figures 5 (a), (b), and (c) represent the specimens without the TiO₂ buffer layer, with the sputtered TiO₂ layer, and the plasma sprayed TiO₂ layer, respectively. The composition of the as-deposited film, Ir:Ru = 9.53 (11.76 wt%:88.24~90.47wt%), was maintained stoichiometric regardless of the type and the presence of the TiO₂ layer,

indicating IrO₂/RuO₂ as the stable oxides.⁵⁾ The top-coat film was analyzed using XRD to identify the preferred orientation as shown in Figure 6. Although the chemical composition of the as-deposited films was almost identical, the enhanced intensity of certain lattice planes ((110), (101), and (211)) in the film having the plasma sprayed TiO₂ layer (Figure 6 (b) ((d))) was not seen in the film having the sputtered TiO₂ layer (Figure 6 (a)) because the microstructure of the TiO₂ buffer layer may affect the growth behavior of the top-coat film,¹⁰⁾ leading to the better anticorrosion properties of the electrode. It is conceivable in the present study that the corrosion resistance depends on the presence and the type of the TiO₂ intermediate layer, indicating that the as-deposited IrO₂-RuO₂ film having the plasma-sprayed TiO₂ layer is the most effective.

4. Conclusions

The optimum process condition of the IrO₂-RuO₂ film on Ti electrodes for the corrosion resistance was evaluated by Taguchi method and orthogonal arrays and determined

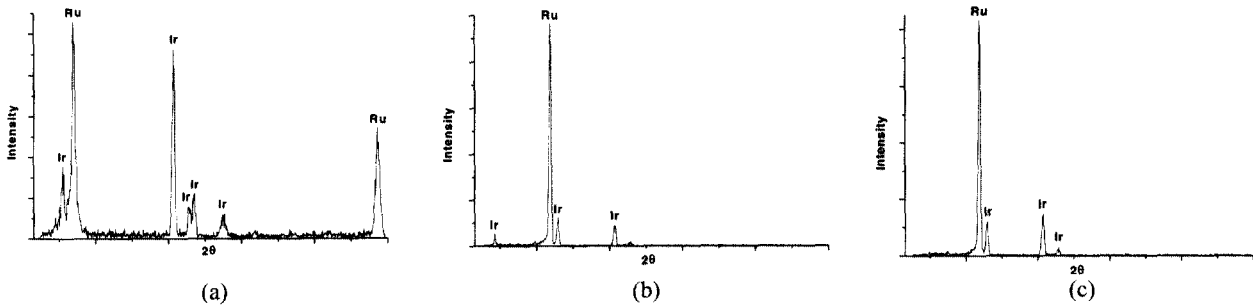


Fig. 5. The EDX analysis of (a) Ti/IrO₂-RuO₂ electrode at an air flow rate of 7 sccm; (b) Ti/TiO₂/IrO₂-RuO₂ electrode having the sputtered TiO₂ layer; (c) Ti/TiO₂/IrO₂-RuO₂ electrode having plasma sprayed TiO₂ layer.

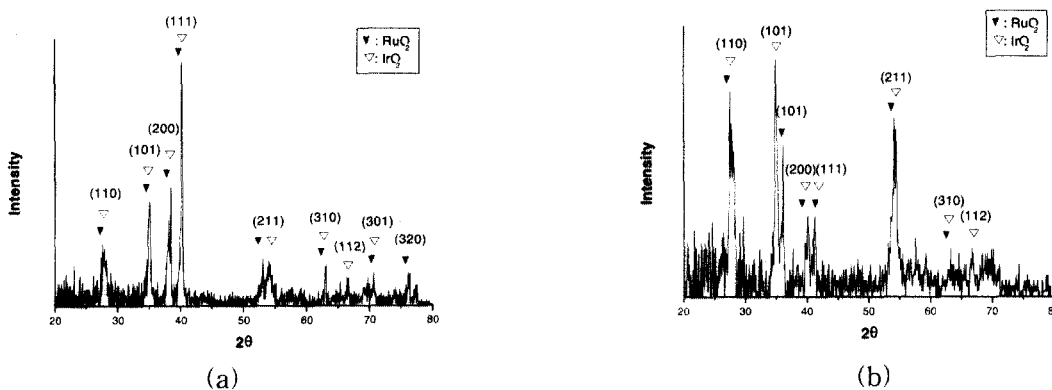


Fig. 6. XRD patterns of specimen (a) specimen no. 4, (b) specimen no. 8.

to be $A_3B_2C_1D_3$. Experimentally, the dip-coated IrO_2 - RuO_2 film was composed of the TiO_2 intermediate layer prepared by plasma spray (A_3) and subsequently heat treated for 120 min (D_3) at $450^\circ C$ (B_2) with 3 sccm flow rate of air (C_1). The current density of the resulting electrode was $0.076 A/cm^2$, representing that it is effective to the corrosion resistance. It could be concluded that the presence and the type of the TiO_2 intermediate layer is dependent on the corrosion properties of the IrO_2 - RuO_2 film on Ti electrode in this system.

References

1. L. Krusin-Elbaum, M. Wittmer, and D. S. Yee, *Appl. Phys. Lett.* **50**(26), 1879 (1987).
2. I. M. REANEY, K. BROOKS, R. KLISSURSKA, C. PAWLACZYK and N. SETTER, *J. Am. Ceram. Soc.* **77**(5), 1209 (1994).
3. D. P. VIJAY and S. B. DESU, *J. Electrochem. Soc.*, **140**(9), 2640 (1993).
4. L. Krusin-Elbaum, M. Wittmer, *J. Electrochem. Soc.* **135**(10), 2610 (1988).
5. L. Krusin-Elbaum, *Thin Solid Films* **169**, 17 (1989).
6. L. A. BURSILL and K. G. BROOKS, *J. Appl. Phys.* **75**, 4501 (1994).
7. R. MRAZ and J. KRYSA, *J. Appl. Electrochem.* **24**, 1262 (1994).
8. H. H. UHLIG and R. W. REVIE, *Corrosion and corrosion control*, p. 48, John Wiley & Sons, Inc., New York, USA, 1985.
9. K. DEHAND, *Quality engineering in production system*, McGraw-Hill Book Co., New York, USA, (1989).
10. S. HORACEK and S. PUSCHAUVER, *Chem. Eng. Prog.* **67**, 71 (1981).